Characterization of Flow-Through Electrode Processes by AC Impedance

C. Y. Yuh
Energy Research Corporation, Danbury, CT 06813

J. R. Selman
Dept. of Chemical Engineering, Illinois Institute of Technology, Chicago, IL 60616

AC-impedance method has been used successfully in characterizing a packed-bed flow-through electrode system. A macrohomogeneous model was developed to simulate the effect of structural, physical and flow parameters. The relative importance of kinetics and mass transfer can be inferred from the AC-impedance analysis. Kinetic information about copper deposition in supported cupric sulfate solution has been obtained successfully using this technique.

Introduction

Flow-through porous electrodes, such as packed-bed and fluidized-bed electrodes, are attractive for electrowinning, electro-organic synthesis and flow-battery applications. The extensive surface area of the porous electrodes makes high volumetric reaction rate more possible than in a cell with smooth electrodes. Forced convection also enhances mass-transfer rate and hence reduces concentration polarization.

In a previous article (Yuh and Selman, 1985), a steady-state analysis was carried out to quantify the relative importance of the various partial-rate processes at a packed-bed electrode where bed depth, flow rate, and electrolyte conductivity were varied. A detailed mathematical model was also developed to aid the analysis. In this article, it is demonstrated that AC-impedance method is a more convenient tool for *in situ* identification of rate-limiting processes in a porous flow-through electrode.

AC-Impedance Method

AC-impedance method has been extensively reviewed by Gabrielli (1981) and Macdonald (1987). In an AC-impedance experiment, a small AC signal is used to perturb the electrochemical system and the response of the system is observed. High-precision measurements may be possible because the response can be averaged over a long run. Using small AC signals also greatly simplifies the theoretical analysis because mass-transfer and kinetic expressions can be linearized at the local polarization and concentration levels. Furthermore, because the various partial-rate processes generally have different time constants, impedance experiments carried out at various frequencies, in many cases, allow assignment of partial-rate processes to different impedance loops (for example, in a fuel cell system studied by Yuh and Selman, 1988 and 1991). Therefore, the dominant rate-limiting processes can often be more easily identified than by other steady-state methods.

A smooth planar electrode can often be represented by an equivalent circuit (Bard and Faulkner, 1980). Similarly, a porous electrode can be represented by a network of equivalent circuits (transmission-line model) (Keiser et al., 1976; Macdonald et al., 1991). In the present work, a differential-equation model was developed to simulate frequency response of a flow-through porous electrode. Such a model is more convenient to use for simulating the behavior of coupled activation and mass-transfer polarizations at different DC polarization levels. A similar model was developed to study fuel-cell electrode processes (Yuh and Selman, 1988).

Macrohomogeneous AC-Impedance Model

A macrohomogeneous model was developed to simulate AC response of a flow-through porous electrode. The model is very general in nature and can also be applied to other porous electrode systems, with modifications. The following assumptions were made:

- The electrode particles and electrolyte are homogeneously mixed as a continuum (see Figure 1). The input parameters are porosity and specific surface area.

Correspondence concerning this article should be addressed to J. R. Selman.

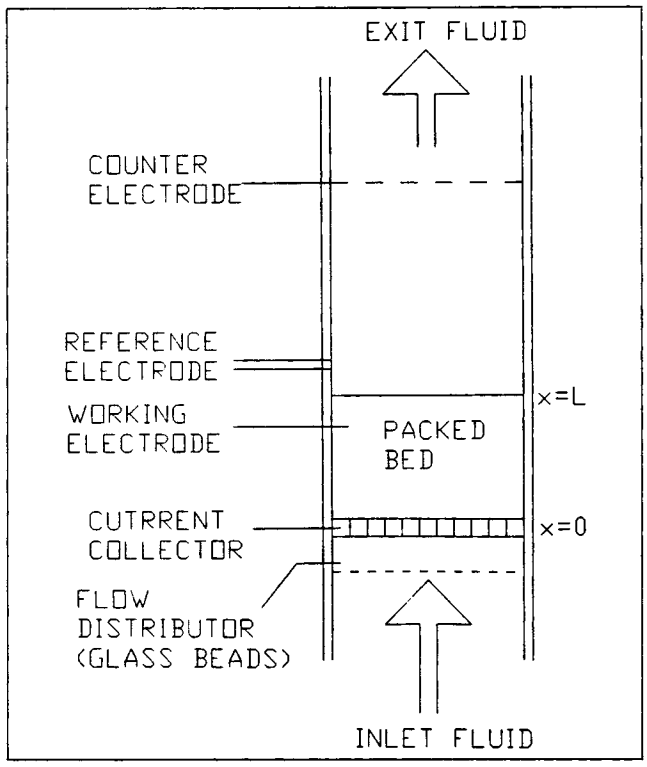

Figure 1. Schematic of flow-through electrode.

- The general Butler-Volmer equation (an electrochemical kinetic expression, see Newman, 1991) is used. The local charge-transfer impedance (that is, the resistance to electrochemical charge-transfer reaction) is characterized by the linearized Butler-Volmer kinetics, as will be shown below.
- The frequency response of the bulk reactant concentration is considered.
- The electronic conductivity of the electrode matrix is high enough to consider it isopotential.
- Ionic transport is represented adequately by ohmic law. Electrolyte migration is considered unimportant, because the liquid phase is well supported by supporting electrolytes.
- The intrinsic activity of the electrocatalyst is uniform throughout the electrode, as are electrochemical kinetic parameters.
- The Warburg (mass-transfer) impedance can be approximated by a Nernst-type expression (Schuhmann, 1966; Gabrielli, 1981); a stagnant diffusion layer approximates the mass-transfer or concentration boundary layer. The resulting local Warburg impedance is then (in the absence of homogeneous chemical reactions):

$$Z_w = \Delta\eta_c / \Delta i_n \tag{1a}$$

$$= G_w + (n^2F\phi)^{-1} \sum_i |S_i| \tanh(q_i\delta)/(\overline{C_{si}} D_{mi} q_i) \tag{1b}$$

The G_w term is for the frequency response of the bulk concentration.

The electrochemical reaction is generally expressed as:

$$\sum_i S_i R_i^{Z_i} \rightarrow ne^- \tag{2}$$

A mass balance for each reactant i yields the following unsteady-state diffusion equation:

$$\epsilon \frac{\partial C_i}{\partial t} + V \frac{\partial C_i}{\partial X} - D_i \frac{\partial^2 C_i}{\partial X^2} = -\frac{S_i a i_n}{nF} \tag{3}$$

A balance on the ionic current in the electrolyte yields the potential equation:

$$K \frac{\partial^2 \Phi}{\partial X^2} + a i_n = -aC_d \frac{\partial \eta_s}{\partial t} \tag{4}$$

The Butler-Volmer kinetics can be linearized with respect to $\overline{\eta_s}$ and $\overline{C_{si}}$, for small perturbations of η_s and C_s:

$$i_n \approx \overline{i_n} + i_o^b \left[\prod_i \left(\frac{\overline{C_{si}}}{C_{Ri}} \right)^{\gamma_i} \right] [\alpha_a \phi \exp(\alpha_a \phi \overline{\eta_s}) + \alpha_c \phi \exp(-\alpha_c \phi \overline{\eta_s})](\eta_s - \overline{\eta_s}) + i_o^b [\exp(\alpha_a \phi \overline{\eta_s}) - \exp(-\alpha_c \phi \overline{\eta_s})] \sum_k \left\{ \gamma_k \left(\frac{\overline{C_{sk}}}{C_{Rk}} \right)^{\gamma_k - 1} \prod_{l \neq k} \left(\frac{\overline{C_{sl}}}{C_{Rl}} \right)^{\gamma_l} \right] (C_{sk} - \overline{C_{sk}}) \Bigg\} \tag{5}$$

The exchange current density, i_o, can be considered as the rate constant for the electrochemical reaction.

If only a small perturbation of current or voltage is applied to the flow-through electrode, the following approximation may be assumed:

$$i_n = \overline{i_n} + \tilde{i}_n = \overline{i_n} + \Delta i_n e^{j\omega t} \tag{6}$$

$$C_i = \overline{C_i} + \tilde{C}_i = \overline{C_i} + \Delta C_i e^{j\omega t} \tag{7}$$

$$\eta_s = \overline{\eta_s} + \tilde{\eta}_s = \overline{\eta_s} + \Delta\eta_s e^{j\omega t} \tag{8}$$

$$\Phi = \overline{\Phi} + \tilde{\Phi} = \overline{\Phi} + \Delta\Phi e^{j\omega t} \tag{9}$$

Therefore, Eq. 5 becomes:

$$\Delta i_n = i_o^o \prod_i (\overline{C_{si}})^{\gamma_i} D_3 \Delta\eta_s + i_o^o D_4 \times \sum_k \left\{ \gamma_k \overline{C_{sk}}^{\gamma_k - 1} \prod_{l \neq k} \overline{C_{sl}}^{\gamma_l} \right\} \Delta C_{sk} \tag{10}$$

or

$$\Delta i_n = i_o^o [D' \Delta\eta_s + D'' \Delta C_s] \quad \text{for a one-reactant system} \tag{11}$$

η_s and Φ are related according to:

$$\eta_s = -\Phi + \frac{RT}{nF} \ln \left[\prod_i \left(\frac{C_{si}}{C_{Ri}} \right)^{S_i} \right] \tag{12}$$

Equation 12 may be simplified to:

$$\eta_s = -\Phi + \frac{1}{n\phi}\sum_i S_i \ln\left(\frac{\overline{C_{si}}}{C_{Ri}}\right) + \frac{1}{n\phi}\sum_i S_i\left(\frac{\tilde{C}_{si}}{\overline{C_{si}}}\right) \tag{13}$$

if $\tilde{C}_{si} \ll \overline{C_{si}}$.

Therefore,

$$\Delta\eta_s = -\Delta\Phi + \frac{1}{n\phi}\sum_i S_i(\Delta C_{si}/\overline{C_{si}}) \tag{14}$$

The last term in Eq. 14 is actually $\Delta\eta_c$.

By substituting Eqs. 1, 6–9, 11 and 14 into Eqs. 3 and 4, with subsequent nondimensionalization, one obtains:

$$\frac{d^2}{d\zeta^2}\Delta\Psi = \underset{\sim}{M}_1\Delta\underset{\sim}{C} + M_2\Delta\Psi \tag{15}$$

$$\frac{d}{d\zeta}\Delta\underset{\sim}{C} + \underset{\approx}{D}\frac{d^2}{d\zeta^2}\Delta\underset{\sim}{C} = \underset{\approx}{P}_1\Delta\underset{\sim}{C} + \underset{\sim}{P}_2\Delta\Psi \tag{16}$$

The boundary conditions are:

$$\zeta = 0 \quad \frac{d}{d\zeta}\Delta\Psi = 0$$

$$\Delta\underset{\sim}{C} - \underset{\approx}{D}\frac{d}{d\zeta}\Delta\underset{\sim}{C} = 0 \tag{17}$$

$$\zeta = 1 \quad \Delta\Psi = 1 - B''\frac{d}{d\zeta}\Delta\Psi$$

$$\frac{d}{d\zeta}\Delta\underset{\sim}{C} = 0 \tag{18}$$

for a system with downstream counter and reference electrodes (Figure 1). The values of $\underset{\sim}{M}_1$, M_2, $\underset{\approx}{P}_1$, $\underset{\sim}{P}_2$ are functions of $\overline{\eta_s}$ and $\overline{C_{si}}$; therefore, steady-state solutions are needed first for determining them.

The impedance, by definition, is:

$$Z = \frac{\Delta\Psi_o}{AK\left.\frac{d}{d\zeta}\Delta\Psi\right|_{\zeta=1}} \tag{19}$$

The system of ordinary differential equations (Eqs. 15 and 16) can be solved by numerical techniques to determine $\Delta\underset{\sim}{C}$ and $\Delta\Psi$ as a function of ζ.

For the flow-through electrode examined here (Cu deposition/dissolution), only one reactant (Cu) is present. The polarization level was carefully controlled to avoid the parasitic hydrogen evolution reaction that could occur at high polarization levels. Therefore, Eqs. 15 and 16 become:

$$\frac{d}{d\zeta^2}\Delta\Psi = m_1\Delta C + m_2\Delta\Psi \tag{20}$$

$$\frac{d}{d\zeta^2}\Delta C + D\frac{d^2}{d\zeta^2}\Delta C = p_1\Delta C + p_2\Delta\Psi \tag{21}$$

If the experiment is performed at open-circuit voltage (OCV) and the axial bulk concentration relaxation can be neglected, the model Eqs. 20 and 21 can be simplified to:

$$\frac{d^2}{d\zeta^2}\Delta\Psi = Q\Delta\Psi, \tag{22}$$

which can be solved analytically.

The solution for Eq. 22 is:

$$Z = R_s + \frac{H\coth(\sqrt{Q})}{\sqrt{Q}} \tag{23}$$

This result is similar to that derived by de Levie (1967). The Nyquist plot for Eq. 23 has been described by Yuh and Selman (1988). Without charge-transfer reaction, the Nyquist plot shows a 45° asymptote at high frequencies and a 90° asymptote at low frequencies. The distance between the 90° asymptote and the imaginary axis is $R_s + H/3$. This distance can be used to estimate effective electrolyte conductivity. In the presence of a charge-transfer reaction, the low-frequency part has to intersect the real axis. Furthermore, the larger the charge-transfer impedance, the smaller the angular frequency at the top of the high-frequency charge-transfer loop. If mass-transfer impedance is included, a second loop at low frequencies occurs which takes off at 22.5°. In spite of the simplicity, Eq. 23 is capable of a complete description of the frequency response of a flow-through electrode at OCV. The values of the exchange current density may be estimated directly from the size of the high-frequency loop.

To solve model Eqs. 20 and 21, numerical techniques are required. Here, orthogonal collocation method was selected. This method has been applied extensively to solving chemical engineering problems (Villadsen and Stewart, 1967; Finlayson, 1974). In the present problem, we selected the Legendre polynomial as a trial function and used the subroutines JACØBI and DFØPR of Villadsen and Michelsen (1978) to calculate the roots of the polynomials and the coefficient matrices. The same orthogonal collocation method was also used to solve the steady-state model equations (Yuh and Selman, 1985).

Copper Deposition in Acidified Solution

In the present work, copper deposition/dissolution in dilute cupric sulfate solution was studied by AC-impedance technique. Such a system has been extensively used as a model system for studying mass transfer and current distribution in flow-through electrode systems (Bennion and Newman, 1972; Newman and Tiedeman, 1978; Yuh and Selman, 1985). The electrochemical kinetics of copper deposition has been reviewed by Yuh and Selman (1985). The mechanism reported by Newman (1991) gives the following theoretical kinetic parameters:

$$\alpha_a = 1.5 \quad \alpha_c = 0.5 \quad \gamma = 0.75$$

γ is the exponent on the concentration term in the electro-

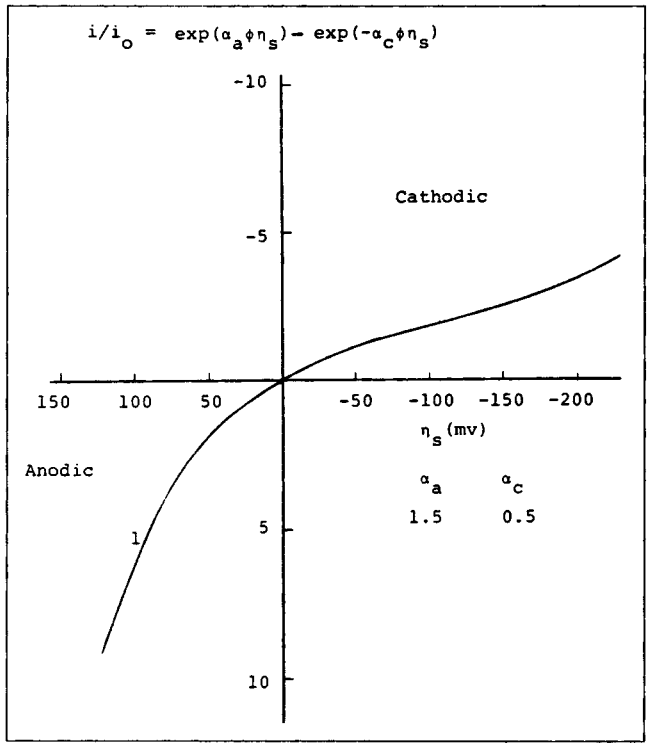

Figure 2. Butler Volmer kinetics ($T = 298$ K).

chemical (Butler-Volmer) kinetic expression (see Eq. 5). The experimentally determined γ value is between 0.42–0.67. Only the theoretical value 0.75 was used here. The value of γ can be determined easily only if the bulk inlet concentration of Cu^{++} was varied during the experiment. In this work, the bulk inlet concentration was fixed at 2 mM.

Figure 2 shows the Butler-Volmer kinetics (with the above kinetic parameters) showing the effect of activation polarization on the local charge-transfer rate. If the electrode is polarized cathodically, its local charge-transfer impedance should become larger first due to the characteristics of the electrode kinetics (see Figure 2). The impedance can become even larger due to the depletion of the reactant because of the corresponding positive reaction order. It is possible for the charge-transfer impedance to become small at very high activation polarization levels; however, for the flow-through electrode studied here, the local charge-transfer impedance would still become large for cases of excessive depletion of Cu^{++} near surface (for example, at limiting current). The bulk concentration of Cu^{++} ion in this work was intentionally kept very low (~ 2 mM) to enhance the mass-transfer impedance so that the experimental system was always under mixed control by charge transfer and mass transfer, for a better demonstration of the AC-impedance technique. For a more concentrated system (for example, 0.1 M Cu^{++}), the mass-transfer impedance would be relatively much smaller than the charge-transfer impedance and the system would be essentially under charge-transfer control only.

On the other hand, if the electrode is polarized anodically, the concentration of the reactant (copper metal) does not decrease. Only the accumulation of Cu^{++} has some effect, but a small one; therefore, the activation overpotential becomes the dominant factor. The anodic transfer coefficient, 1.5, is

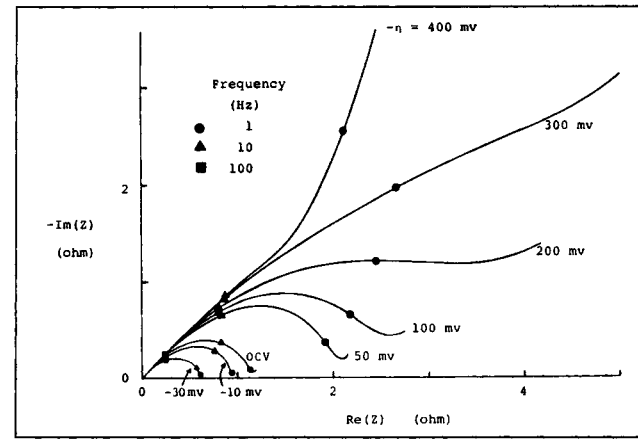

Figure 3a. Predicted frequency response of a flow-through electrode at various DC polarization levels.

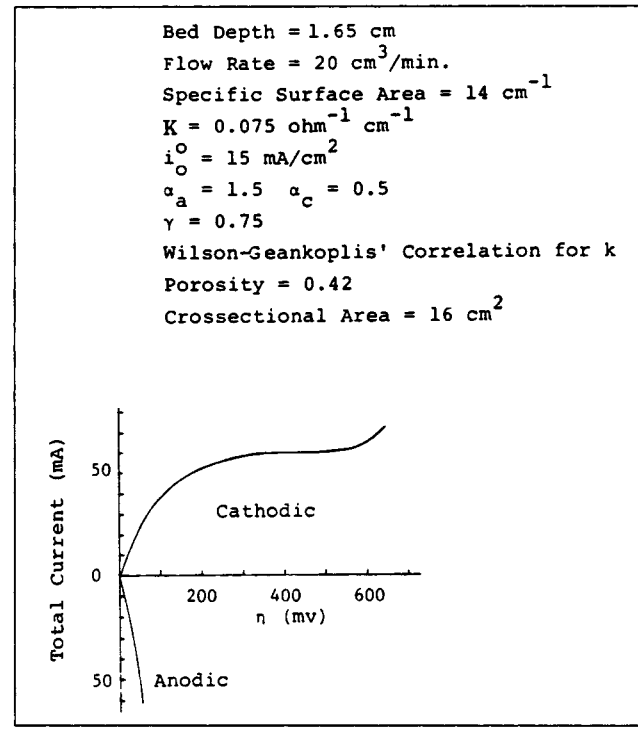

Figure 3b. Input conditions and steady-state polarization for Figure 3a.

larger than the cathodic transfer coefficient, 0.5. The local charge-transfer impedance would most probably decrease due to this effect (see Figure 2).

Figure 3a demonstrates the effect of steady-state polarization on the impedance generated by solving Eqs. 20 and 21 using orthogonal collocation method, for some typical parameters of a flow-through electrode (with sodium sulfate as the supporting electrolyte). The steady-state polarization curve, Figure 3b, was generated first, by solving the model equations described in the previous article (Yuh and Selman, 1985). The mass-transfer correlation given by Wilson and Geankoplis (1986) (applicable to low Re and high Pe systems):

Table 1. Characteristics of the Flow-Through Electrode System

Cathode: Copper Shot [~1/8 in. (~3.2 mm) dia.] or Copper-Coated Steel [1/8 in. (~3.2 mm) dia.]

Anode: Copper Screen

Reference Electrode: Copper Rod

Electrolyte: 2 mM $CuSO_4$ (analyzed by Atomic Absorption) and 0.8 M Na_2SO_4 or 1.5 M H_2SO_4

Anode Reaction: Copper Dissolution
Cathode Reaction: Copper Deposition, Hydrogen Evolution

Solution Properties

	Supporting Electrolyte	
	Na_2SO_4	H_2SO_4
Density, g/cm^3	1.098	1.088
Viscosity, cm^2/s	1.22×10^{-2}	1.22×10^{-2}
Conductivity, ohm$^{-1}\cdot$cm^{-1}	0.074–0.085	0.5
Diffusivity Cu^{++}, cm^2/s	6×10^{-6}	7.6×10^{-6}

Re: 0.1–40
Pe: 200–80,000

$$\frac{\epsilon d_p k}{D_m} = 1.09\left(\frac{v d_p}{D_m}\right)^{1/3} \tag{24}$$

was used to calculate k, the average mass-transfer coefficient. The diffusion-layer thickness, δ, is estimated from:

$$\delta = \frac{D_m}{k} \tag{25}$$

for the calculation of the local Warburg impedance (Eq. 1).

If the flow-through electrode is polarized cathodically, the impedance increases. When the limiting current is approached, the local charge-transfer impedance becomes so large (because of the very low Cu^{++} concentration near the surface) that the total impedance approaches that without a charge-transfer reaction. Moreover, at the limiting current (but without hydrogen evolution), the reactant concentration near surface is so small that the local Warburg impedance also becomes very large (according to Eq. 1a). Therefore, a 90° asymptote at low frequencies is predicted.

If the electrode is polarized anodically, the impedance becomes smaller. The local charge-transfer and Warburg impedances both decrease as the reactant concentration near surface increases. The calculated frequency response is in agreement with these qualitative expectations.

The AC response of the bulk concentration profiles calculated from the macrohomogeneous impedance model indicates that the frequency response of the bulk concentration can be neglected under the experimental conditions used in this study. Only at very low frequencies (below about 0.01 Hz) or liquid flow rates significantly lower than those used in this study, an additional loop corresponding to the bulk concentration appears, because the time constant of the bulk concentration relaxation is usually very large. Above 0.1 Hz, the frequency response of the bulk concentration needs not be considered; therefore the model Eq. 21 can be dropped to simplify the calculation.

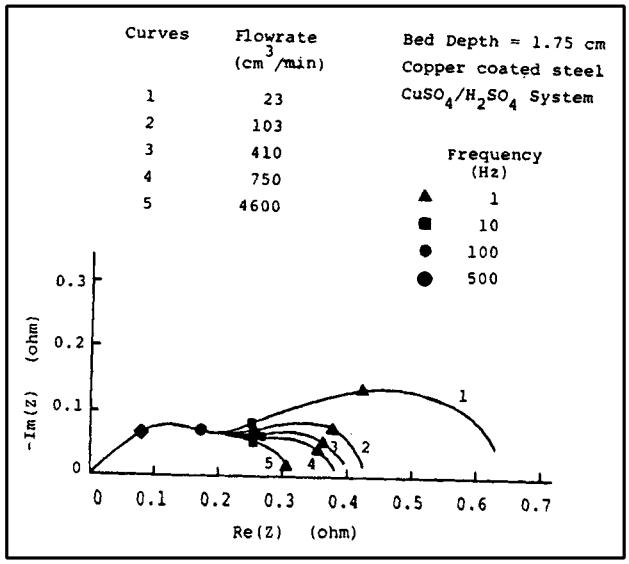

Figure 4. Effect of liquid flow rate on measured frequency response at open circuit.

Experimental Method

The electrochemical system studied here is copper deposition/dissolution in dilute acidic cupric sulfate solution. The experimental setup is the same as that described in the previous publication (Yuh and Selman, 1985). The important characteristics of the system are given in Table 1. If sodium sulfate was used as the supporting electrolyte, the pH was adjusted to a value between 2.3–2.4 by addition of sulfuric acid. The DC polarization was kept below that which would initiate hydrogen evolution reaction. The AC-impedance experiment was carried out under a variety of flow rates and polarization levels. The bed depth was also varied. The equipment used included a Stonehart BC1200 potentiostat and a Solartron 1172 Frequency Response Analyzer. The impedance measurements were carried out potentiostatically at about 15 frequencies between 0.1 Hz and 5 KHz. On the Nyquist diagrams shown in this article, only data points at four typical frequencies (1, 10, 100, and 500 Hz) were plotted. A small AC signal (<9.5 mV peak-to-peak) was used to perturb the system.

Qualitative Discussion

The effect of the liquid flow rate on the frequency response at OCV is shown in Figure 4. The high-frequency loop is not affected by the flow rate, since the local charge-transfer impedance is uniform at OCV. Furthermore, the mass-transfer impedance can be neglected at higher frequencies. On the other hand, the size of the low-frequency loop decreases with respect to the flow rate, indicating that the mass-transfer coefficient increases with the flow rate. These observations are in agreement with the qualitative predictions.

The mass-transfer coefficient determined from the size of the mass-transfer loop is found to be much lower (more than one order of magnitude lower) than the Wilson-Geankoplis' prediction (Eq. 24) which applies at the limiting current. On the other hand, the mass-transfer coefficient at limiting current, determined in the previous study using only the steady-

state data, was found very close to the Wilson-Geankoplis' prediction (Yuh and Selman, 1985). The mass-transfer coefficient at limiting current cannot be determined easily from the impedance data because there is no distinct low-frequency impedance loop for estimating it. A complicated nonlinear least-square fitting of data in the whole frequency range is required and was not attempted in this work.

There may be several reasons why the estimated mass-transfer coefficient differs from the one determined at the limiting current:

- The simple stagnant diffusion layer is not a suitable approximation of the boundary layer, since mixing and developing convection are typical for a flow-through electrode. Therefore, the frequency response of such a complicated boundary layer with attachment and detachment may not be correctly simulated by the simple Nernst theory.
- The mass-transfer coefficient at OCV may be different from that at the limiting current where the Wilson-Geankoplis' correlation applies. This may be due to the very different concentration boundary layers at the different polarization levels. There is no fundamental reason why mass-transfer coefficient measured at the limiting current should be applicable below the limiting current (Newman and Tiedmann, 1978). For example, mass-transfer boundary layer at OCV has been found to be about 70% thicker than at limiting current (Anantharaman et al., 1989), for natural convection at a vertical wall.
- Surface diffusion of adions may become rate-limiting at low overpotentials, as opposed to charge-transfer rate-limiting at high overpotentials (Bockris and Reddy, 1970). Surface diffusion limitation may have caused the large low-frequency loop at OCV which cannot be explained by the liquid-phase mass-transfer coefficient.
- The possibility of rate-limiting step for charge-transfer as $Cu^+ + e^- \rightarrow Cu$ near OCV (as opposed to $Cu^{++} + e^- \rightarrow Cu^+$ at higher overpotentials) was reported by Erdey-Gruz, 1972. The liquid-phase diffusion of intermediate Cu^+ ion and the homogeneous reaction $Cu^{++} + Cu \rightarrow 2Cu^+$ may need to be considered.

In conclusion, more detailed study is required to clarify this low-frequency impedance results, particularly near OCV.

The experimental AC-impedance decreases with anodic polarization (see Figure 5) and increases with cathodic polarization (see Figures 6–10). This is consistent with the qualitative discussion and model predictions. As the limiting current is approached, the impedance approaches the predicted results for very large charge-transfer impedance. However, a faster approach to the predicted results for very large charge-transfer impedance is observed in the case of sulfuric acid as the supporting electrolyte (Figures 8–10). If the supporting electrolyte is sodium sulfate, the true limiting current cannot be easily approached even at very large polarization levels (for example, 400 mV), due to its lower electrolyte conductivity. However, if the supporting electrolyte is sulfuric acid, the true limiting current can be easily reached. In other words, a planar electrode approximation can be approached more easily if the solution conductivity is higher (de Levie, 1967); the penetration depth increases with increasing solution conductivity.

The experimental data also showed that the impedance below the limiting current was smaller if sulfuric acid was used as the supporting electrolyte (comparing Figures 6 and 8), expected from its lower electrolyte ohmic resistance. In addition,

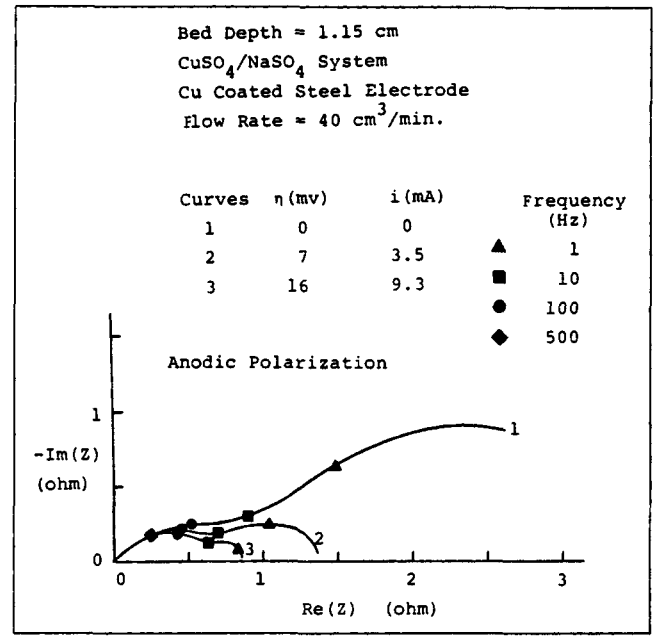

Figure 5. Effect of anodic polarization on measured frequency response.

the 90° asymptote is closer to the imaginary axis with increasing solution conductivity (comparing Figures 7 and 10), also expected (Yuh and Selman, 1988).

If the flow rate is increased, the effect of the steady-state polarization on the impedance decreases (see Figure 7). The larger the mass-transfer coefficient, the less the extent of the depletion of the surface concentration of Cu^{++} while the electrode is polarized. The larger the surface concentration, the smaller the charge-transfer and mass-transfer impedances.

Below the limiting current, bed depth has very little effect on the impedance. This is because the electrode cannot approach the planar electrode approximation for bed depths such as 1.15–2.35 cm used in this study. Unless a much smaller bed depth is used, the effect of the bed depth is unimportant. However, at the limiting current, the local impedance becomes so large that the planar electrode approximation may be approached. In other words, the larger the local impedance, the larger the penetration depth (de Levie, 1967).

Quantitative Analysis of Experimental Data

If aL^2/K is very large (that is, the reaction zone is restricted to part of the packed-bed near the current collector), the solution of the simplified impedance model (Eq. 23) can be reduced to:

$$Z \simeq \frac{H}{\sqrt{G}} \tag{26}$$

The kinetic loop can be expressed by the following equations:

$$\text{Real Part} = \frac{\sqrt{\cos\theta'}\,\cos(\theta'/2)}{A\sqrt{a\phi i_o^b K(\alpha_a + \alpha_c)}} + R_s \tag{27}$$

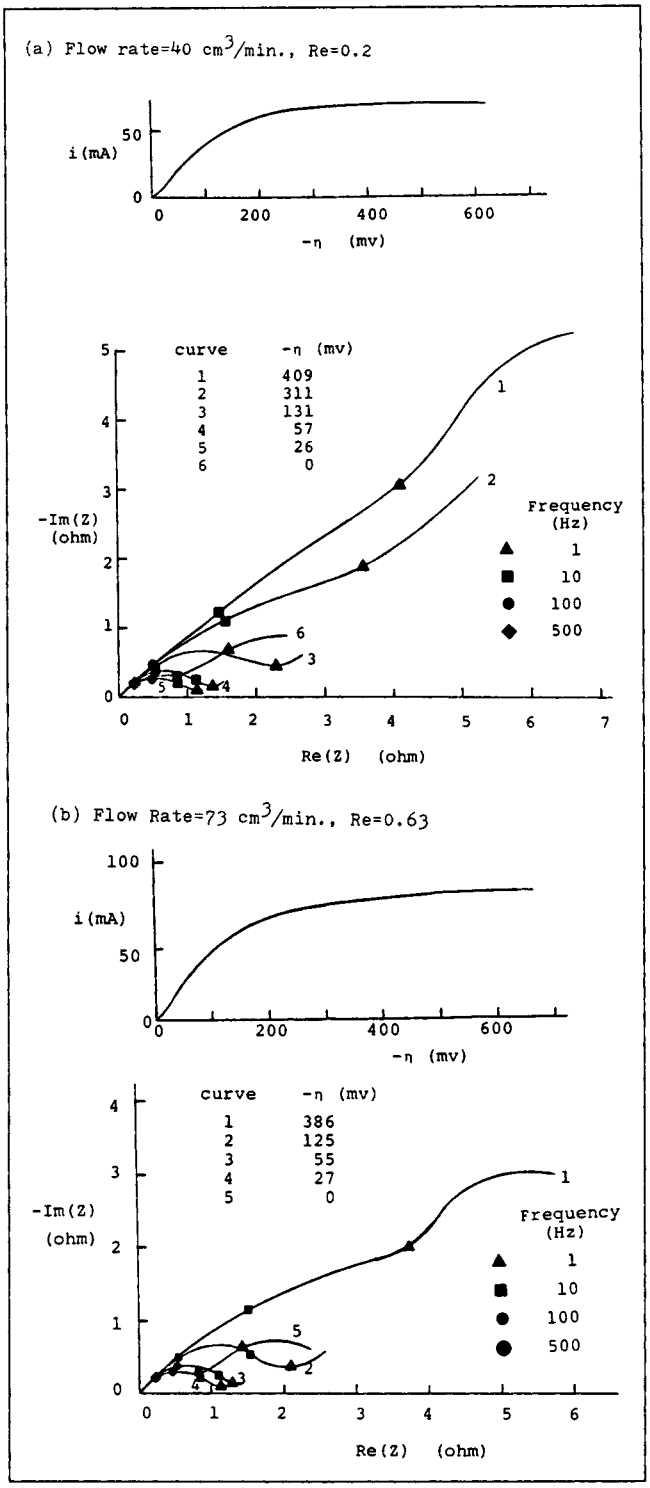

Figure 6. Experimental impedance results at various flow and cathodic polarization levels (Cu-coated steel; $CuSO_4/Na_2SO_4$ system; bed depth = 1.15 cm).

$$\text{Imaginary Part} = \frac{\sqrt{\cos\theta'}\,\sin(\theta'/2)}{A\sqrt{a\phi i_o^b K(\alpha_a+\alpha_c)}} \qquad (28)$$

where $\theta' = \tan^{-1}(\omega C_d/A')$.

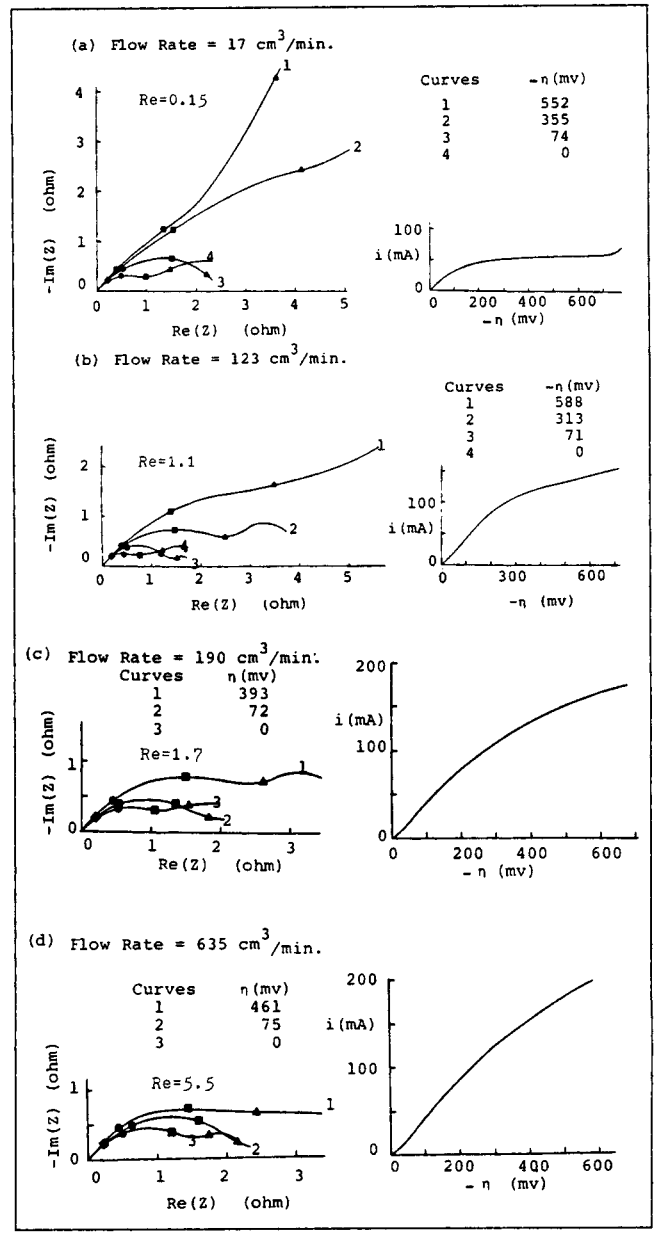

Figure 7. Experimental impedance results at various flow and cathodic polarization levels (Cu-coated steel; $CuSO_4/Na_2SO_4$ system; bed depth = 1.65 cm) (frequency (Hz): ▲ 1 ■ 10 ● 100 ◆ 500).

The quantities $i_o^b Ka$ and C_d/i_o^b can be obtained by a nonlinear least-square regression of the real and imaginary parts of the high frequency loops by Eqs. 27 or 28. The independent variables are frequency and R_s. A nonlinear regression program, using Newton-Raphson algorithm, was used to search the extremum. The effective conductivity of the packed bed can be estimated from the distance between the 90° asymptote and the imaginary axis, characterizing the impedance data at the limiting current.

Several estimated parameters from the nonlinear regression analysis are shown in Tables 2 and 3. The exchange current density for copper deposition seems to be smaller with sodium sulfate as the supporting electrolyte, if γ is assumed the same

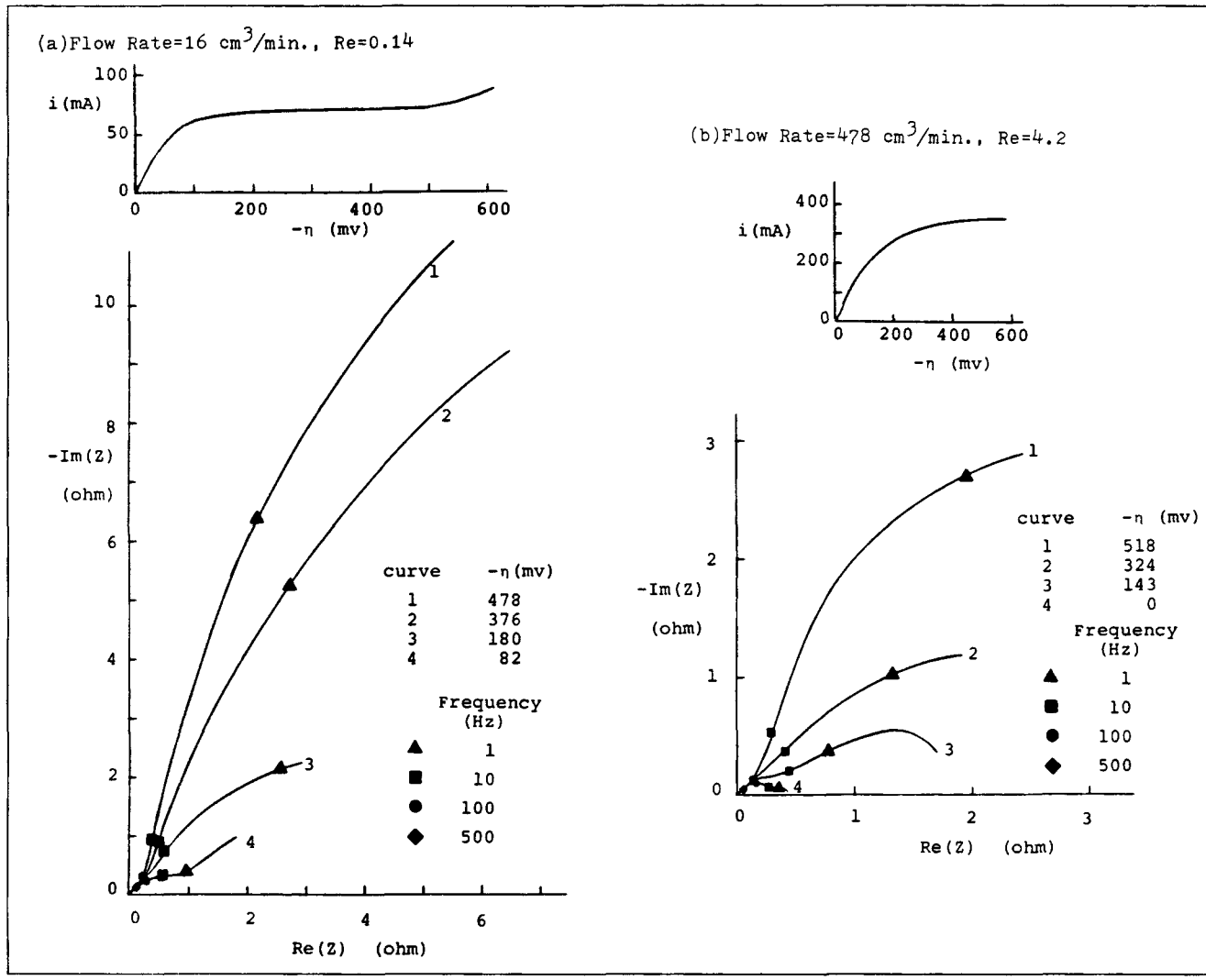

Figure 8. Experimental impedance results at various flow and cathodic polarization levels (Cu-coated steel; $CuSO_4/H_2SO_4$ system; bed depth = 1.2 cm).

for both supporting electrolytes. The standard exchange current density is usually slightly higher than the values by the steady-state fitting (Yuh and Selman, 1985), if γ is assumed to have the theoretical value 0.75. This may indicate that the value of γ may be smaller than 0.75. To accurately determine the value of γ, solutions of various Cu^{++} concentrations are recommended in the experiments. The effective electrolyte conductivity of the packed-bed with sulfuric acid as the supporting electrolyte is in very good agreement with the theoretical value (0.127 ohm^{-1} cm^{-1}). The estimated double layer capacitance is between 60 and 90 $\mu F/cm^2$ with sulfuric acid and about 70 $\mu F/cm^2$ with sodium sulfate.

The experimental data can also be analyzed by fitting the data with the complete macrohomogeneous model. The fitting procedure is very complicated: The steady-state data have to be fitted first by the steady-state model. The local impedance distribution is then calculated from the steady-state concentration and the potential profiles. Finally, the AC-impedance data is fitted by the macrohomogeneous AC-impedance model. The adjustable parameters are specific surface area, mass-transfer coefficient, exchange current density, effective conductivity, transfer coefficients α_a and α_c, and γ, and double-layer capacitance.

Since there are so many adjustable parameters, a complete fit requires a detailed nonlinear least-square regression analysis. Furthermore, a detailed understanding of the frequency response of the mass-transfer boundary layer at various polarization levels (not available so far) is required for an adequate fit. Therefore, only a set of AC-impedance data was fitted, using theoretical parameters (α_a, α_c and γ) and mass-transfer coefficient according to Wilson and Geankopolis, without using a least-square regression analysis. It should be noted that this fit is very preliminary in nature and a complete fit of all experimental data is meaningful only after an adequate model of the mass-transfer boundary layer at various polarization levels becomes available.

The fitted results are shown in Figure 11. The standard exchange current density determined is about 10 mA/cm^2, which is of the same order of magnitude as those determined by the fitting of the steady-state data. The double layer ca-

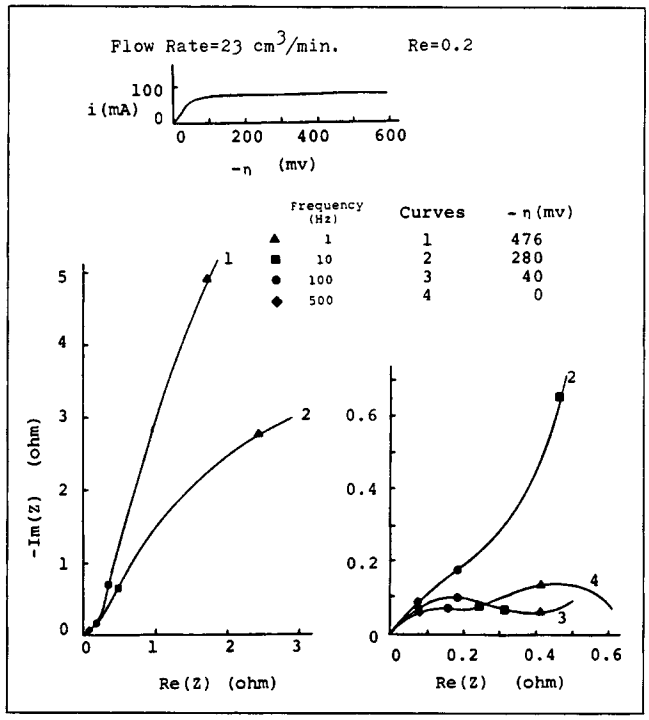

Figure 9. Experimental impedance results at various cathodic polarization levels (Cu-coated steel; $CuSO_4/H_2SO_4$ system; bed depth = 1.75 cm).

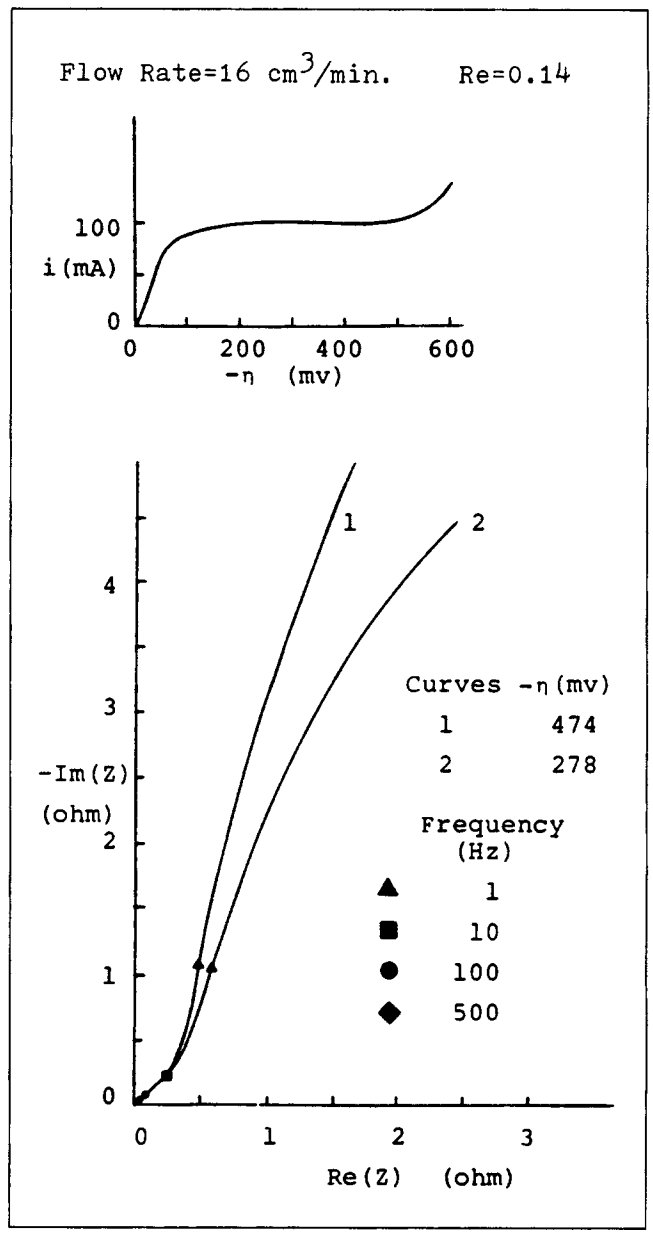

Figure 10. Experimental impedance results at various cathodic polarization levels (Cu shot; $CuSO_4/H_2SO_4$ system; bed depth = 2.35 cm).

pacitance determined is about 70 $\mu F/cm^2$, very close to that determined by regression analysis of the open circuit data (see Table 2).

Conclusions

- The general characteristics of a packed-bed flow-through electrode can be simulated successfully by a macrohomogeneous AC-impedance model. The effects of the effective conductivity, specific surface area, electrode kinetics, double layer charging, mass transfer, and DC polarization on the frequency response can be reasonably predicted by the model. The simplified version requires far less effort and yields adequate accuracy for most practical purposes.
- The higher the flow rate, the smaller the mass-transfer impedance. The kinetic loop at open circuit is not affected by the liquid flow rate. The mass-transfer coefficient at open

Table 2. Kinetic Parameters Estimated by Nonlinear Regression Analysis of Experimental Data (Supporting Electrolyte Na_2SO_4)

System	1	2
Bed depth, cm	1.15	1.65
i_o^b, mA/cm^2	0.26	0.16
C_d, μF/cm^2	72	74
i_o^o, mA/cm^2, γ = 0.75	27	17
[Cu^{++}], mM	2	2
Fixed Parameters		
K = 0.02 ohm$^{-1}\cdot$cm^{-1}		
a = 14 cm^{-1}		

Table 3. Estimated Kinetic Parameters from Nonlinear Regression Analysis of Experimental Data (Supporting Electrolyte H_2SO_4)

System	1	2	3
Bed Depth, cm	1.2	1.75	2.35
Packing Particle	Cu/Steel	Cu/Steel	Cu Shot
i_o^b, mA/cm^2	0.373	0.604	0.478
K, l/ohm·cm	0.125	0.124	0.131
C_d, μF/cm^2	88	75	60
[Cu^{++}], mM	2	3	2.6
i_o^o, mA/cm^2; γ = 0.75	39	47	41
Fixed Parameters			
a = 15 cm^{-1}			

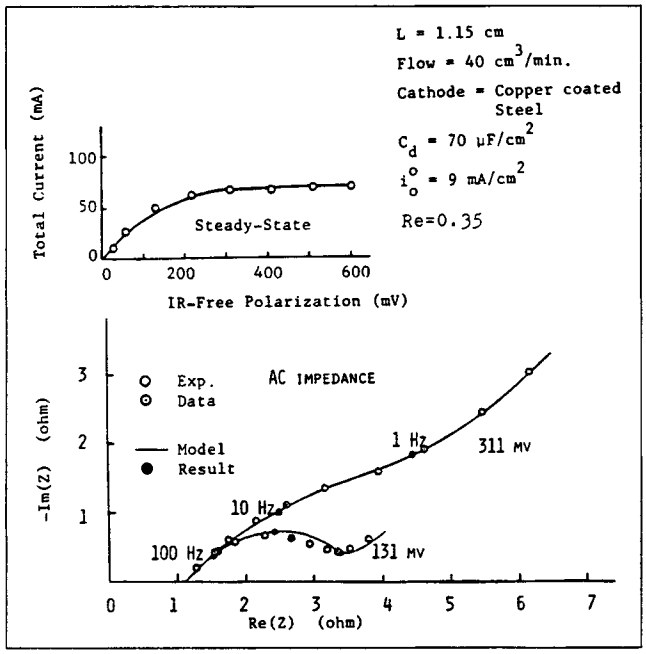

Figure 11. Fitting of experimental AC-impedance results.

circuit seems to be smaller than that at the limiting current. The frequency response characteristics of the mass-transfer boundary layer in the packed-bed electrode system cannot be explained adequately by the simple theory of Nernst diffusion layer.

- The steady-state polarization level has a very large effect on the frequency response. The impedance increases with cathodic polarization, due to the effect of the depletion of Cu^{++} near the electrode surface, which dominates over the characteristics of the Butler-Volmer kinetics (see Figure 2). The impedance decreases with anodic polarization, due to the constant activity of the reactant (copper metal) which does not affect the characteristics of the electrode kinetics.
- The exchange current density determined is of the same order of magnitude as those determined by fitting the steady-state data.
- The double layer capacitance of the copper electrode determined by the nonlinear regression analysis is about 70 $\mu F/cm^2$.

Acknowledgment

This work was supported by the Electric Power Research Institute, Palo Alto, CA, under Contract No. RP-1085-2. The general research support from the Institute of Gas Technology, Chicago, and the typing of this manuscript by Energy Research Corporation are also appreciated.

Notation

a = specific surface area, cm^{-1}
$a_1 = \epsilon j\omega L/V$
$a_2 = i_o^o D_3 \prod_i (\overline{C_{si}})^{\gamma_i}$
$a_3 = a\phi L^2/K$
$a_4 = -aj\omega C_d \phi L^2/K$
$a_5 = -1 - A_1 A_{10}$
$a_6 = a_2 a_5 - A_3 A_{10}$
A = cross-sectional area of flow-through electrode, cm^2
$A' = i_o^b \phi(\alpha_a + \alpha_c)$
A_1 = vector $[B_i]$, $B_i = S_i/(n\phi\overline{C_{si}})$
A_2 = vector $[B_i]$, $B_i = S_i aL/(VC_{Ri}nF)$
A_3 = vector $[B_i]$, $B_i = \gamma_i \overline{C_{si}}^{\gamma_i - 1} \prod_{\substack{l \\ l \neq i}} (\overline{C_{sl}})^{\gamma_l}$
$A_4 = I - A_6 A_3$
A_5 = matrix $[B_{ij}]$, $B_{ij} = 0$ if $i \neq j$, $B_{ij} = [\cosh(q_i\zeta)]^{-1}$ if $i = j$
A_6 = vector $[B_i]$, $B_i = a_2 S_i \tanh(q_i\zeta)/(q_i nFD_{mi})$
$A_7 = A_6 A_1$
$A_8 = A_4 - A_7$
$A_9 = (A_8)^{-1} A_5$
$A_{10} = (A_8)^{-1} A_6$
$A_{11} = A_1 A_9$
$A_{12} = a_2 A_{11} + A_3 A_9$
A_{13} = matrix $[B_{ij}]$, $B_{ij} = 0$ if $i \neq j$, $B_{ij} = \overline{C_{Ri}}$ if $i = j$
$B'' = AR_s K/L$
C = bulk concentration, mol/cm^3
C_i = bulk concentration of species i, mol/cm^3
C_{si} = surface concentration of species i, mol/cm^3
C_{Ri} = reference concentration of species i, mol/cm^3
$\Delta\underset{\sim}{C}$ = vector $[B_i]$, $B_i = \Delta C_i/C_{Ri}$
C_d = double-layer capacitance, $Farad/cm^2$
d_p = particle diameter, cm
$D = \epsilon(D_a + D_m)/(VL)$
D_{mi} = molecular diffusivity of species i, cm^2/s
$D_1 = \exp(\alpha_a \phi \overline{\eta_s})$
$D_2 = \exp(-\alpha_c \phi \overline{\eta_s})$
$D_3 = \alpha_a \phi D_1 + \alpha_c \phi D_2$
$D_4 = D_1 - D_2$
$D' = D_3 \overline{C_s}^{\gamma}$
$D'' = \gamma \overline{C_s}^{\gamma - 1} D_4$
$D_i = \epsilon(D_a + D_{mi})$
$D_a = 3V(1-\epsilon)/(a\epsilon)$, axial dispersion coefficient, cm^2/s
$\overline{D_i} = D_i/(VL)$
$\underset{\approx}{D}$ = matrix $[B_{ij}]$, $B_{ij} = 0$ if $i \neq j$, $B_{ij} = \overline{D_i}$ if $i = j$
F = Faraday constant
$G = (aL^2/K)(A' + j\omega C_d)$
$G_w = (RT/nF) \sum_i \{\Delta C_i/[\overline{C_{si}} \cosh(q_i\zeta)]\}$
$H = L/(aK)$
i_n = transfer current density, mA/cm^2
i_o^b = bulk exchange current density, mA/cm^2
i_o^o = standard exchange current density, mA/cm^2
I = matrix $[B_{ij}]$, $B_{ij} = 0$ if $i \neq j$, $B_{ij} = 1$ if $i = j$
Im = imaginary part
$j = \sqrt{-1}$
k = mass-transfer coefficient, cm/s
K = effective electrolyte conductivity, $ohm^{-1} \cdot cm^{-1}$
L = bed depth, cm
m_1 = single-reactant representation of $\underset{\sim}{M}_1$
m_2 = single-reactant representation of $\underset{\sim}{M}_2$
$\underset{\sim}{M}_1 = (-a_3 A_{12} + a_4 A_{11}) A_{13}$
$\underset{\sim}{M}_2 = (-a_3 a_6 + a_4 a_5)/\phi$
n = number of electron transferred
OCV = open circuit voltage or equilibrium potential
p_1 = single-reactant representation of $\underset{\approx}{P}_1$
p_2 = single-reactant representation of $\underset{\sim}{P}_2$
$\underset{\approx}{P}_1 = aA_{13} - A_2 A_{12} A_{13}$
$\underset{\sim}{P}_2 = -a_6 A_2/\phi$
P_e = Peclet number, $V/(aD_m)$
$Q = aL^2 Z_1/K$
$q_i = \sqrt{(j\omega)/D_{mi}}$
R = universal gas constant
R_e = real part or Reynolds number $[V/(a\nu)]$
R_i = reactant i
R_s = solution resistance, ohm; outside the flow-through electrode
S_i = stoichiometric coefficient of species i
T = temperature, °K
V = superficial fluid velocity, cm/s

X = axial distance, cm
Z = total impedance, ohm
Z_i = charge of species i
Z_l = local impedance, $(A' + j\omega C_d)/(1 + Z_w A')$
Z_w = local Warburg (mass-transfer) impedance, ohm·cm^2

Greek letters

α_a = anodic transfer coefficient
α_c = cathodic transfer coefficient
γ_i = reaction order of species i
δ = diffusion layer thickness, cm
Δ = AC part of a signal
ϵ = porosity
ζ = X/L
η_c = concentration polarization, V
η_s = activation polarization, V
ν = kinematic viscosity, cm^2/s
ϕ = $F/(RT)$
Φ = electrolyte potential, V
Φ_o = externally applied voltage, V
Ψ = $\phi\Phi$
Ψ_o = $\phi\Phi_o$
ω = angular frequency

Superscripts

~ = AC part
- = average

Literature Cited

Anantharaman, V., P. N. Pintauro, and L. Nanis, "Analysis of Convective Mass Transfer by Potential Relaxation. I. Steady-state Copper Deposition with Laminar Natural Convection Stirring," *J. Electrochem. Soc.*, **136**, 1727 (1989).

Bard, A. J., and L. R. Faulkner, *Electrochemical Methods: Fundamentals and Applications*, Wiley, New York (1980).

Bennion, D. N., and J. Newman, "Electrochemical Removal of Copper Ions from Very Dilute Solutions," *J. Applied Electrochem.*, **2**, 113 (1972).

Bockris, J. O'M, and A. K. N. Reddy, *Modern Electrochemistry*, Plenum Press, New York (1970).

Erdey-Gruz, T., *Kinetics of Electrode Processes*, Wiley-Interscience, New York (1972).

Finlayson, B. A., "Orthogonal Collocation in Chemical Reaction Engineering," *Cat. Rev.-Sci.*, **10**, 69 (1974).

Gabrielli, C., *Identification of Electrochemical Processes by Frequency Response Analysis*, Monograph Reference 004/83, Solartron Instrument Group, Farnsborough, England (1981).

Keiser, H., K. D. Deccu, and M. A. Gutjahr, "Abschatzung der Porenstruktur Poroser Elektroden aus Impedanzmessunchen," *Electrochim. Acta*, **21**, 539 (1976).

de Levie, R., "Electrochemical Responses of Porous and Rough Electrodes," *Adv. Electrochem. Electrochem. Eng.*, **6**, 329 (1967).

Macdonald, D. D., M. Urquidi-Macdonald, S. D. Bhakta, and B. G. Pound, "The Electrochemical Impedance of Porous Electrodes in Alkaline Media, II: Nonuniform Transmission Line Analysis," *J. Electrochem. Soc.*, **138**, 1359 (1991).

Macdonald, J. R., *Impedance Spectroscopy*, Wiley, New York (1987).

Newman, J., *Electrochemical Systems*, 2nd ed., Prentice-Hall, Englewood Cliffs, NJ (1991).

Newman, J., and W. Tiedemann, "Flow-Through Porous Electrodes," *Adv. Electrochem. Electrochem. Eng.*, **11**, 353 (1978).

Schuhmann, D., "Sur l'impédance de Diffusion en Basse Fréquence," *Comptes Rendus*, **262C**, 624 (1966).

Villadsen, J. V., and M. L. Michelsen, *Solution of Differential Equation Models by Polynomial Approximation*, Prentice-Hall, Englewood Cliffs, NJ (1978).

Villadsen, J., and W. E. Stewart, "Solution of Boundary-Value Problems by Orthogonal Collocation," *Chem. Eng. Sci.*, **22**, 1483 (1967).

Wilson, E. J., and C. J. Geankoplis, "Liquid Mass-Transfer at Very Low Reynolds Numbers in Packed Beds," *Ind. Eng. Chem. Fund.*, **5**, 9 (1966).

Yuh, C. Y., and J. R. Selman, "Polarization Behavior of Packed-Bed Electrodes: A Comparative Study of Experimental and Modeling Results," *Chem. Eng. Commun.*, **38**, 135 (1985).

Yuh, C. Y., and J. R. Selman, "Characterization of Fuel Cell Electrode Processes by AC-Impedance," *AIChE J.*, **34**, 1949 (1988).

Yuh, C. Y., and J. R. Selman, "The Polarization of Molten Carbonate Fuel Cell Electrodes, II. Characterization by AC Impedance and Response to Current Interruption," *J. Electrochem. Soc.*, **138**, 3649 (1991).

Manuscript received Nov. 4, 1991, and revision received Nov. 25, 1992.